J Mater Sci: Mater Med (2009) 20:889–896
DOI 10.1007/s10856-008-3631-y

An asymmetric coating composed of gelatin and hydroxyapatite for the delivery of water insoluble drug

Junwu Xiao · Yingchun Zhu · Yanyan Liu · Yi Zeng · Fangfang Xu

Received: 29 February 2008 / Accepted: 16 October 2008 / Published online: 20 November 2008

Abstract An asymmetric coating composed of gelatin and hydroxyapatite on Ti6Al4V alloy implant was prepared to control the release of water-insoluble drug ibuprofen and improve the surface properties of the implant. The asymmetric coating developed into a thin dense outer layer and a thick porous inner layer using a dip-coating method and a succedent phase-inversion process. The drug loading ranged from 10 to 30% (w/w), and depended on the immersion time and drug concentration in the quenching solution. The in vitro release from this system was always at an approximately zero-order rate and at least lasted for 30 days. The in vitro studies in SBF revealed that the coating could induce the formation of apatite, and was fully covered after 14 days soaking in SBF solution. This asymmetric coating had better bioactivity of inducing the formation of apatite in vitro, compared with pure gelatin coating and bare Ti6Al4V implant.

1 Introduction

Recently, titanium and its alloys are found increasing application in surgical implants due to the biocompatibility and fatigue strength [1]. However, clinical evidences revealed some problems as metal ions detected in tissues close to implants and the bio-inert surfaces [2]. Moreover, infection in an implant context is prevalent and clinically difficult to treat. Conventional therapy with systemic antibiotics is expensive, prone to complications and often unsuccessful. Therefore, controlled antibiotics release systems in combination with implants have been developed to circumvent these problems. Recently interests are stimulated in coating implant with the bioactive, biodegradable materials and antibiotics to improve the surface properties and reduce the infection rate [3–6].

In search of bioactive and biodegradable materials coating on implants, collagen, gelatin and calcium phosphate have received much attention because of their special properties [7–9]. Collagen and apatite are the two primary components of extracellular bone matrix. Gelatin is the denatured state of collagen, which possesses arginine–glycine–aspartic acids (RGD) sequences reported to stimulate the adhesion of osteoblastes and improve the osteointegration [10, 11]. Calcium phosphate, such as hydroxyapatite (HAp), tricalcium phosphate (TCP) and so on, were proved having bioactive properties and thus improving the bonding strength on bone tissue, without inducing the growth of fiber tissue [12].

Drug loaded films are widely applied in pharmaceutical technology. Numerous controlled or sustained delivery systems have been developed, whereby the active ingredients have been dissolved or dispersed within films [13, 14]. In these systems, drugs are usually released in a typical bi-phasic fashion: an initial burst release followed by a long, tail of low and largely incomplete release [14, 15]. It is well known that persistent low drug concentration, below the minimal inhibitory concentration (MIC) values surrounding an implant, may cause the development of resistant bacteria [16, 17]. Therefore, the perfect release mode is to maintain the drug concentration steady over the MIC value before releasing completely. Drug delivery systems based on the principles of osmosis have been shown to exhibit precise, zero-order kinetics in a variety of

J. Xiao · Y. Zhu (✉) · Y. Liu · Y. Zeng · F. Xu
Shanghai Institute of Ceramics, Chinese Academy of Science, Shanghai 200050, China
e-mail: yzhu@mail.sic.ac.cn

applications, including the asymmetric coating for the delivery of water insoluble drug [18].

In this study, we developed an asymmetric coating composed of gelatin and hydroxyapatite on Ti6Al4V alloy implant for using as a drug-delivery system and improving the surface properties of the implant. The in vitro release behavior and bioactivity of this system were evaluated. The in vitro release was constant release kinetics and a longer than 1-month delivery lifetime. A layer of bioactive apatite fully covered on the initial surface after 14 days soaking in SBF solution.

2 Experimental

2.1 Materials

Calcium nitrate tetrahydrate ($Ca(NO_3)_2 \cdot 4H_2O$, AR), diammonium hydrogen phosphate ($(NH_4)_2HPO_4$, AR), ammonium hydroxide ($NH_3 \cdot H_2O$, 25–28%), polyethylene glycol 2000 (PEG-2000), gelatin, hydrofluoric acid (HF, ≥40%), nitric acid (HNO_3, 65.0–68.0%), anhydrous ethanol (AR), acetone (AR), glutaraldehyde solution ($C_5H_8O_2$, 25%) and ibuprofen were purchased from Sinopharm Chemical Reagent Co., Ltd. All reagents are used without further purification.

2.2 Preparation of hydroxyapatite nanoparticles

Hydroxyapatite nanoparticles were prepared through chemical precipitation. Firstly, solution (a) was prepared containing 0.5 M $Ca(NO_3)_2$, 1% (W/W) PEG-2000, and its pH was adjusted to 10.0 using ammonium hydroxide. Solution (b) was prepared with 0.5 M $(NH_4)_2HPO_4$ and the pH was adjusted to 10.0 using ammonium hydroxide. Secondly, solution (b) was added in a drop-wise fashion into solution (a) with vigorous stirring. The Ca/P ratio was set to 1.67. The precipitates were aged for 3 h at room temperature and then separated from the mother liquor by filtration. Thirdly, the precipitates were washed with distilled water by 3 times and then with anhydrous ethanol by 2 times. Finally, the precipitates were dried in the oven at 333 K until the constant weight.

2.3 Preparation of the asymmetric coating

Ti6Al4V alloy plates as substrates (50 mm × 20 mm × 1 mm) were abraded with silicon carbide (SiC) papers (grit range of 400–4,000). Prior to apply coating, samples were ultrasonically cleaned with acetone, ethanol and distilled water for 15 min. Then, they were etched in a mixture of 2 ml of HF and 4 ml of HNO_3 in 1,000 ml of water for 10 min to form a fresh titanium oxide surface. The dipping solution was prepared as follow: 1.00 g of hydroxyapatite was homogenously dispersed into 50 ml of deionized water by using an Ultrasonic Cell Disrupter System (Ningbo Scientz Biotechnology CO., LTD). Next, 10.00 g of gelatin was dissolved into above solution at 313 K, and then sonicated until trapped air bubbles were removed to form the dipping solution.

Asymmetric coatings were prepared through a dip-coating method followed by a phase inversion process. Firstly, substrates were immersed into the dipping solution for several minutes and then drawn out at the constant speed under 313 K bath. Secondly, the coatings were dried in an air for several minutes and then immersed into a quenching solution composed of anhydrous ethanol and ibuprofen for several days. Thirdly, the coatings were cross-linked through glutaraldehyde, and later repeatedly washed by deionized water and anhydrous ethanol. Finally they were dried at 313 K until the constant weight. Five samples have been prepared with different experimental parameters shown in Table 1.

2.4 In vitro ibuprofen release

The in vitro study of ibuprofen release was determined by ultraviolet spectroscopy, using a U-3010 spectrophotometer (Hitachi High-Technologies Co., Ltd). Samples were soaked in 20 ml pH = 7.32 SBF solution at 310 K, proposed by Kokubo et al. [19] The release medium was withdrawn at predetermined time intervals, and replaced

Table 1 The experiment parameters of samples

Sample	The drug concentration (mg/ml)	Dried time in air (h)	The immersion time in the quenching solution (days)	The drug loading (W/W %)
A	40	0.5	4	30.98
B	40	1	4	30.49
C	20	0.5	4	10.42
D	30	0.5	4	21.81
E	40	0.5	2	18.74

with fresh soaking medium each time. The analysis was carried out by measuring the absorbance at 264 nm.

2.5 Theoretical considerations

For drug delivery systems that release drug by osmotic pressure, the volumetric flux of water form the surrounding aqueous medium into the device core is given by [20]:

$$\frac{\mathrm{dV}}{\mathrm{d}t} = \frac{A}{h} L_p \sigma \Delta\pi \tag{1}$$

where $\mathrm{d}V/\mathrm{d}t$ is the volumetric influx rate of water into the device core, A is the surface area of the capsule, h is the wall thickness, L_p is the filtration coefficient, σ is the reflection coefficient, and $\Delta\pi$ is the osmotic pressure difference across the wall. The zero-order release rate during the initial portion of the release profile is given by:

$$\frac{\mathrm{d}M}{\mathrm{d}t} = \frac{\mathrm{d}V}{\mathrm{d}t} S \tag{2}$$

where $\mathrm{d}M/\mathrm{d}t$ is the release rate, $\mathrm{d}V/\mathrm{d}t$ is given by Eq. 1, and S is the concentration of the component in the fluid being pumped. If the capsule contains only one component, the osmotic pressure difference is caused by a saturated solution of the component on one side of the capsule wall and sink conditions (assumed) outside the capsule walls. Also, assuming ideality, the expression for $\Delta\pi$ can be written as:

$$\Delta\pi = MRT = \frac{S}{M.W.} RT \tag{3}$$

where R is the universal gas constant, T is the temperature, $M.W.$ is molecular weight, and S is the saturation solubility of the single component (drug). Substituting for $\Delta\pi$ into Eq. 2, the following relation is obtained:

$$\frac{\mathrm{dM}}{\mathrm{d}t} = \left(\frac{A}{h} L_p \sigma RT\right) \frac{S^2}{M.W.} \tag{4}$$

Equation 4 indicates that a plot of the release rate versus $(S/M.W.)$ should be linear with a slope given by the expression in parentheses. Based on Eq. 4, the water permeability (L_p) of the asymmetric membrane capsule wall was calculated.

2.6 In vitro studies in SBF

The in vitro studies in SBF was carried out by soaking the samples vertically in 50 ml SBF solution at 310 K, proposed by Kokubo et al. [19]. The SBF solution was changed every day in the vitro studies and lasted for 21 days.

2.7 Characterization

The phases of the asymmetric coating before and after soaking in SBF solution and the precipitates were characterized by X-ray diffraction (XRD) patterns recorded on D/max 2550 V diffractometer with Cu Kα radiation ($\lambda = 1.542$ Å). The component distributions and the morphologies of the asymmetric coating before and after soaking in SBF solution were studied by scanning electron microscopy coupled with energy dispersive spectroscopy (SEM-EDS) in a JSM-6700F with an accelerating voltage of 10.0 kV. As for the sample preparation for SEM observation, coatings were firstly stripped from substrates for observing the coating surface, and then broken up in liquid nitrogen environment for observing the cross-section of the coating. The morphology of hydroxyapatite was obtained by transmission electron microscopy (TEM) on a JEM-2010 microscope with an accelerating voltage of 200.0 kV.

3 Results and discussion

3.1 Hydroxyapatite nanoparticles

Figure 1 shows the XRD pattern and the morphology of the precipitates obtained through chemical precipitation. The XRD pattern shows that the precipitates are hydroxyapatite

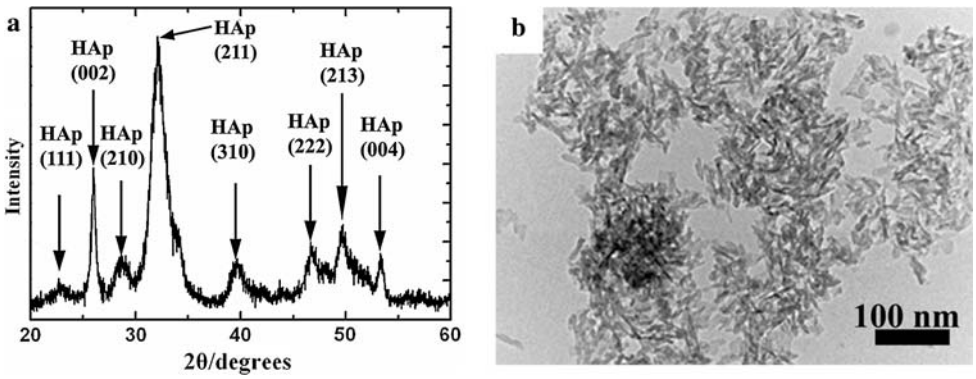

Fig. 1 **a** XRD pattern and **b** TEM image of hydroxyapatite particles

(Fig. 1a), in accordance with the typical pattern of hydroxyapatite (JCPDS 25-0166). The morphology of hydroxyapatite powders is uniform nano-rods with length of 30–50 nm and diameter of 10–15 nm (Fig. 1b). In the preparation process, polyethylene glycol 2000 as dispersant prevents hydroxyapatite nano-rods from agglomeration.

3.2 Asymmetric coating

SEM images of the asymmetric coating are showed in Fig. 2. The asymmetric coating about 130 μm thick is composed of a thin dense outer layer about 10 μm thick and a thick porous inner layer (Fig. 2a and b). The structure of the coating depends on the immersion time in the quenching solution, sample A immersed in the quenching solution for 4 days is significantly more porous than sample E for 2 days, as shown in Fig. 2a and c. Hydroxyapatite nanoparticles are homogenously dispersed in the coating, as seen by Fig. 2d.

The formation of the asymmetric coating is a result of phase-inversion process [21–23]. Gelatin is soluble in warm water as solvent over 313 K and insoluble in anhydrous ethanol as non-solvent. A dense layer is formed by evaporation of solvent in a quiescent air. A porous layer is formed due to the phase inversion by water-ethanol exchange in the quench environment. Besides, the long immersion time in the quenching solution obviously increases the porosity of the coating, as revealed by Fig. 2a and c.

3.3 Study of the drug loading

The drug loading is dependant on the immersion time and drug concentration in the quenching solution. When the coating immerses in the quenching solution to induce phase-inversion, ibuprofen in the quenching solution will diffuse into the coating due to the concentration difference between external and internal of the coating. Although ibuprofen is poorly water-soluble drug, it is easily soluble in anhydrous ethanol. So the drug loading can be adjusted through changing the drug concentration in the quenching solution, as suggested by that the drug loadings are 30.98, 21.81 and 10.42% when the drug concentrations are 40, 30 and 20 mg/ml respectively (Table 1). Furthermore, the drug loading is related with the immersion time in the quenching solution. More drug are loaded in the coating with the immersion time prolonging, as shown by that the drug loading in sample A immersed in the quenching solution for 4 days is 30.98%, higher than 18.74% in sample E for 2 days (Table 1).

3.4 In vitro ibuprofen release

The mass of ibuprofen released to SBF solution versus time is plotted for sample A and B (Fig. 3). All experiment parameters of sample A and B are the same except the dried time in an air. The dried time of sample A in an air is 30 min, less than 60 min in sample B, resulting in the thinner dense layer. As for the in vitro release of sample A,

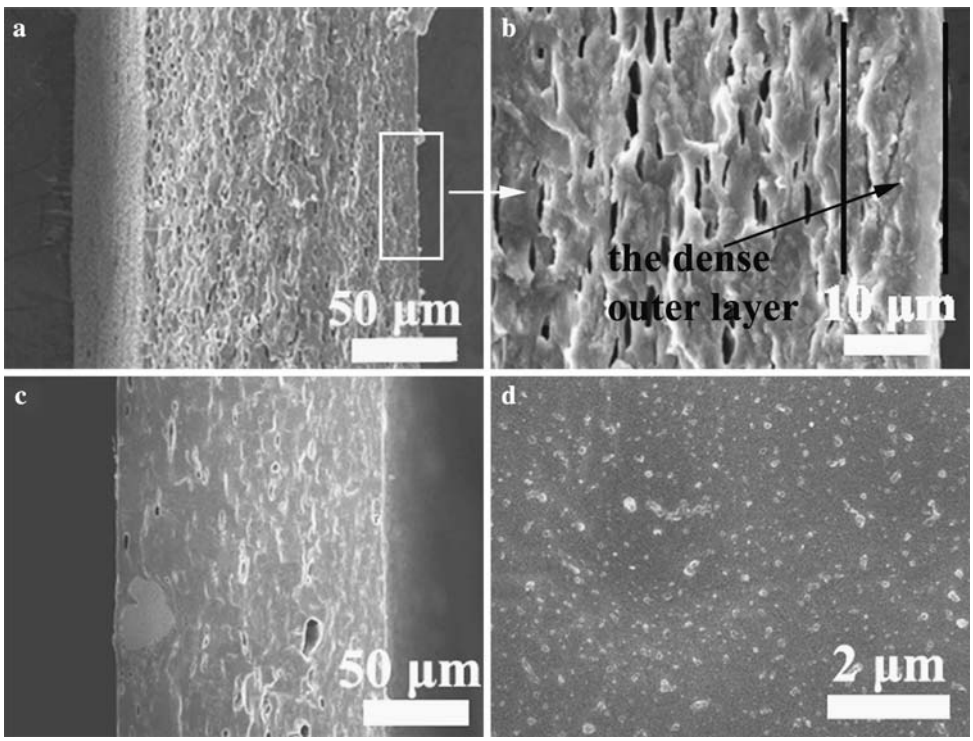

Fig. 2 SEM images of **a** the cross-section of sample A, **b** the thin dense outer layer in sample A, **c** the cross-section of sample E and **d** the surface of sample A

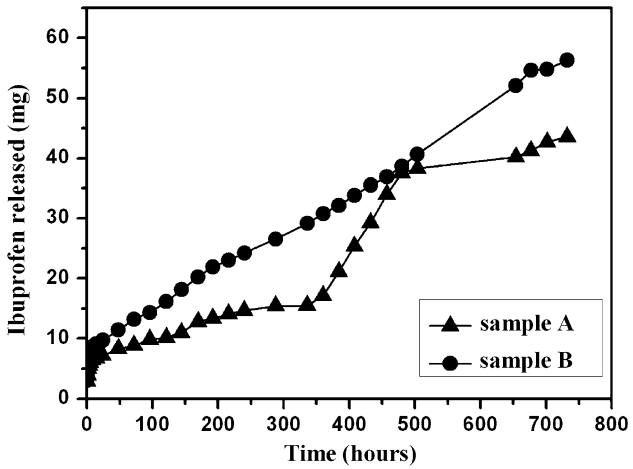

Fig. 3 The in vitro release curves of sample A and B in 20 ml SBF solution within 30 days at 313 K (▲: sample A; ●: sample B)

the release rate is almost constant within the first 14 days. In the period of the 15th ∼ the 20th day, although ibuprofen is released at a constant rate, the release rate obviously becomes fast. After that, the release is a long, tail of low and largely incomplete release. However, the in vitro release from sample B is always zero-order release kinetics and at least lasts for 30 days.

The in vitro release of ibuprofen from an asymmetric coating is zero-order release kinetics, which is revealed by the theoretical calculation and the in vitro release results. On the one hand, many studies reported that drug release from an asymmetric coating is mainly controlled by the osmotic effect for water soluble drug or insoluble drug [18, 20, 24–26]. When the driving force of the release is osmotic pressure, the release rate should be constant revealed by Eq. 4 as long as the saturation solubility of drug and the drug molecular weigh are determined. On the other hand, the in vitro release study of sample B shows that the asymmetric coating releases ibuprofen at an approximately zero-order rate (Fig. 3). In addition, the in vitro release curve of sample A also reveals that the release rate almost keeps unchanged within the first 14 days in SBF solution (Fig. 3). The release rate becomes fast with prolonging the immersion time (Fig. 3). It can be explained by that the dense layer gradually become thin due to the degradation of gelatin with the immersion time prolonging, and the release rate is inverse proportion to the wall thickness according to Eq. 4. With the increase of the immersion time, the dense layer becomes thin, and some parts even rupture, as proved by SEM images of the asymmetric coating surface at various immersion time (Fig. 4). Therefore, ibuprofen is almost released completely in this period. Subsequently, the release of ibuprofen may be controlled by the diffusion-controlled process rather than osmotic pressure. Thus, the release is a long, tail of low and largely incomplete release after 20 days immersing in SBF, similar to the release behavior of the diffusion-controlled process at the end of the release process [27].

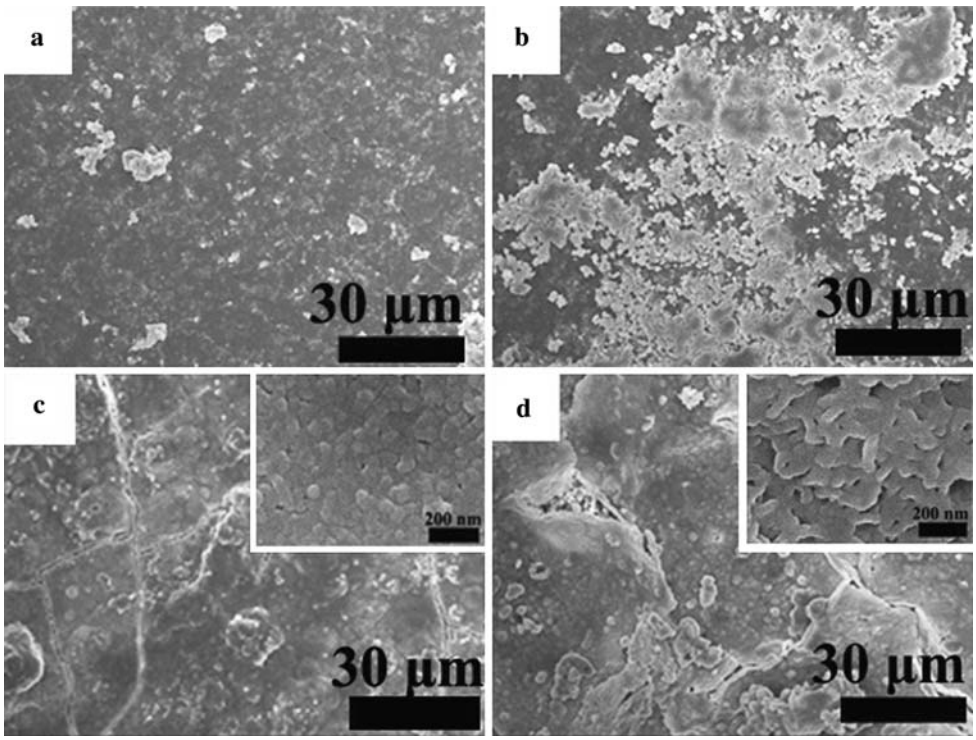

Fig. 4 SEM images of the coating surface immersed in SBF solution at various time, **a** 3 days, **b** 7 days, **c** 14 days and **d** 21 days (Inset: the magnification image)

3.5 In vitro studies in SBF

SEM images of coating surfaces at various soaking time in SBF solution are shown in Fig. 4. After 3 days soaking in SBF solution, a few particles are formed on the local area of the initial surface (Fig. 4a). Most of the initial surface is covered by deposits after 7 days in SBF solution (Fig. 4b). When the immersion time rises to 14 days, the initially surface is totally covered by a layer of deposition. High magnification SEM observation shows that the deposits are composed of nanoparticles about 50–100 nm (Fig. 4c). Upon immersion time for 21 days, spherically shaped particles about 1–10 μm have fully covered on the initial surface and the layer of deposition has ruptured. These micro-sized particles are composed of needle-shaped crystalline aggregate, which can be seen under a higher magnification (Fig. 4d).

EDS analysis of coating surfaces after soaking in SBF solution allows to determine the relative contents (in mol%) of calcium and phosphorous. It suggests that the calcium and phosphorus contents increase with the immersion time in SBF solution prolonging (Fig. 5). After 3 days soaking in SBF solution, the calcium and phosphorus contents are 6.98 and 4.65% respectively, and the Ca/P ratio is 1.50. 7 days later, the amounts are 8.14% Ca and 5.34% P, and the Ca/P ratio is 1.52. After 14 days immersion, there are 14.19% Ca and 8.97% P on the coating surface, and the Ca/P ratio is 1.58. The calcium and phosphorus contents rise to 14.52 and 9.08%, and the Ca/P ratio is 1.60 at the end of the in vitro test (21 days).

SEM-EDS results indicate the varieties in the morphology and composition of coating surfaces after soaking in SBF solution. An increase in calcium and phosphorus contents is observed as the immersion time in SBF solution prolongs, which can be regarded as the deposition of calcium phosphate. The calcium and phosphorous contents significantly increase before 14 days in SBF solution, while such differences become low as the soaking time exceeds 14 days. The results demonstrate that after immersing in SBF solution, a calcium phosphate layer is formed, and fully covered on the initial surface after 14 days soaking in SBF solution, which is in accordance with SEM images of coating surfaces (Fig. 4). The Ca/P ratio gradually increases to 1.60 after soaking in SBF solution for 21 days close to that of bone apatites [27–29]. In addition, some researches reported that no obvious calcification was observed in pure gelatin coating after immersing in SBF solution for 15 days and no apatite was formed on the untreated Ti6Al4V surface even for 8 weeks [30, 31]. Therefore, the in vitro studies in SBF reveal that the composite coating is better bioactivity than pure gelatin coating and bare Ti6Al4V implant.

XRD patterns of the asymmetric coatings before and after immersing in SBF solution for different times are shown in Fig. 6. Before soaking in SBF solution, a broad peak in the range of 15°–25° should belong to gelatin. And some peaks at 31°–33°, 47° and 49° can be ascribed to hydroxyapatite doped in the coating. With the increase of immersion time in SBF, the intensity of gelatin peak

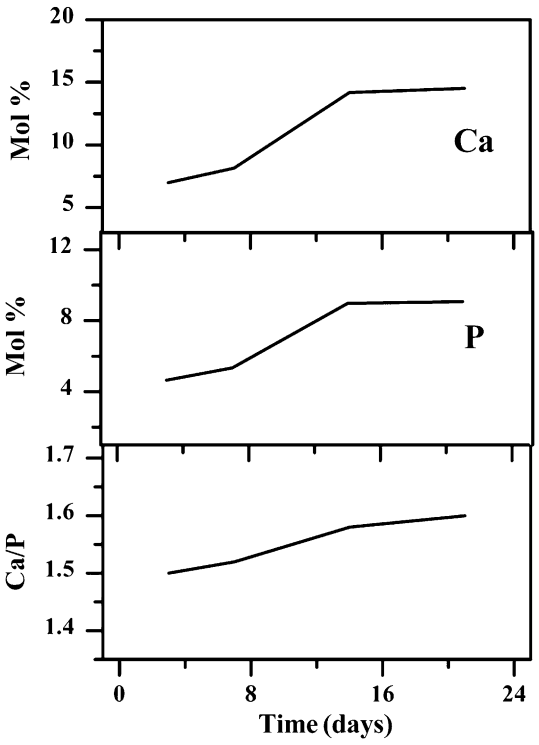

Fig. 5 Relative calcium, phosphorous content (mol%) and Ca/P on the coating surface versus SBF soaking time, as determined by EDS analysis

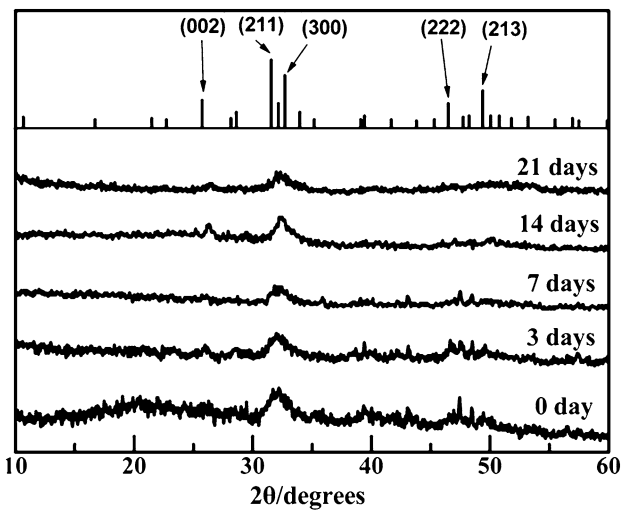

Fig. 6 XRD patterns of the asymmetric coating before and after soaking in SBF for different time periods. A standard XRD pattern of hydroxyapatite is included for reference purposes

gradually becomes weak. After 14 days soaking in SBF solution, a broad peak (15°–25°) of gelatin disappears, which illustrates that other materials gradually accumulate on the initial surface. A peak at $2\theta = 26°$ becomes evident which could be assigned to the (002) reflection of an apatite-like phase when the sample is immersed in SBF solution for a long time. However, the peaks appearing between 45° anf 50° that belonged to hydroxyapatite are gradually decreasing with the time increasing in SBF, which may be caused by the low crystallinity of apatite deposited on the coating surface.

Recently, some vivo studies suggested that the apatite-formation ability was a critical factor in facilitating the chemical fixation of biomaterials to bone tissue, and ultimately affecting the in vivo success of the bone grafting materials [32, 33]. In this study, the results show that the asymmetric coating composed of gelatin and hydroxyapatite could induce the formation of apatite layer on the surface, and is better bioactivity than pure gelatin coating and bare Ti6Al4V implant. Moreover, a few in vivo studies also reported that gelatin and hydroxyapatite were totally degradable, perfectly biocompatible and significantly enhanced the alkaline phosphatase activities and osteocalcin expressed by the cells [34, 35]. In addition, some studies revealed that the osteoblastic cells attached to the HA/gelatin composites to a significantly high degree and subsequently proliferated more, the improvement of the properties may be caused by the less—crystallized and small-sized apatite crystals [35]. Therefore, we have reason to believe that this hydroxyapatite/gelatin composite coating may significantly improve the bioactivity and biocompatible in vivo, compared with bare Ti6Al4V alloy implants.

4 Conclusions

In this study, an asymmetric coating composed of gelatin and hydroxyapatite was prepared on Ti6Al4V alloy implant to use as a drug-delivery system and improve the surface properties of the implant through a dip-coating method followed by a phase inversion process. The drug loading was dependant on the immersion time and drug concentration in the quenching solution. The in vitro release was always at an approximately zero-order rate and at least lasted for 30 days. The results of the in vitro bioactivity experiments revealed that this asymmetric coating could induce the formation of apatite, and was fully covered after 14 days soaking in SBF solution. And this coating showed better bioactivity, compared with pure gelatin coating and bare Ti6Al4V implant. All of these results suggested that this asymmetric coating might be used as a drug release system to prevent inflammation, and as a bioactive, biodegradable layer to induce the formation of apatite and actively bond to the surrounding tissue in vivo.

Acknowledgment The research was partially financially supported from the Nation Natural Science of China (20571082, 50772125), the Science and Technology Commission of Shanghai (08JC1420700), and the National High Technology Research and Development Program of China.

References

1. M. Shirkhanazadeh, J. Mater. Sci.: Mater. Med. **3**, 322 (1992). doi:10.1007/BF00705362
2. G. Meachim, F.D. Williams, J. Biomed. Mater. Res. **1**, 555 (1973). doi:10.1002/jbm.820070607
3. J.S. Price, A.F. Tencer, D.M. Arm, G.A. Bohach, J. Biomed. Mater. Res. **30**, 281 (1996). doi :10.1002/(SICI)1097-4636(199603)30:3<281::AID-JBM2>3.0.CO;2-M
4. H. Gollwitzer, K. Ibrahim, H. Meyer, W. Mittelmeier, R. Busch, A. Stemberger, J. Antimicrob. Chemother. **51**, 585 (2003). doi:10.1093/jac/dkg105
5. M. Lucke, G. Schmidmaier, S. Sadoni, B. Wildemann, R. Schiller, N.P. Haas, M. Raschke, Bone **32**, 521 (2003). doi:10.1016/S8756-3282(03)00050-4
6. M. Aviv, I. Berdicevsky, M. Zilberman, J. Biomed. Mater. Res. Part A **83A**, 10 (2007). doi:10.1002/jbm.a.31184
7. Y.W. Fan, K. Duan, R.Z. Wang, Biomaterials **26**, 1623 (2005). doi:10.1016/j.biomaterials.2004.06.019
8. L. Pang, Y. Hu, Y. Yan, L. Liu, Z. Xiong, Y. Wei, J. Baj, Surf. Coat. Technol. **201**, 9549 (2007). doi:10.1016/j.surfcoat.2007.04.035
9. S.H. Li, Z.G. Zheng, Q. Liu, J.R. De Wijn, K. De Groot, J. Biomed. Mater. Res. **40**, 520 (1998). doi :10.1002/(SICI)1097-4636(19980615)40:4<520::AID-JBM2>3.0.CO;2-H
10. A.S.G. Curtis, J.V. Forrester, J. Cell Sci. **71**, 17 (1984)
11. E. Ruoslahti, M.D. Pierschbacher, Science **238**, 491 (1987). doi:10.1126/science.2821619
12. P. Ducheyne, Q. Qiu, Biomaterials **20**, 2287 (1999). doi:10.1016/S0142-9612(99)00181-7
13. S. Radin, P. Ducheyne, Biomaterials **28**, 1721 (2007). doi:10.1016/j.biomaterials.2006.11.035
14. M. Stigter, J. Bezemer, K. De Groot, P. Layrolle, J. Control. Release **99**, 127 (2004). doi:10.1016/j.jconrel.2004.06.011
15. J. Andersson, S. Areva, B. Spliethoff, M. Linden, Biomaterials **26**, 6827 (2005). doi:10.1016/j.biomaterials.2005.05.002
16. H. Wahlig, E. Dingeldein, Acta Orthop. Scand. **51**, 49 (1980)
17. M.H. Wilcox, T.G. Winstanley, R.C. Spencer, J. Antimicrob. Chemother. **33**, 431 (1994). doi:10.1093/jac/33.3.431
18. C.Y. Wang, H.O. Ho, L.H. Lin, Y.K. Lin, M.T. Shen, Int. J. Pharm. **297**, 89 (2005)
19. T. Kokubo, F. Miyaji, H.M. Kim, T. Nakamura, J. Am. Ceram. Soc. **79**, 1127 (1996). doi:10.1111/j.1151-2916.1996.tb08561.x
20. Y.K. Lin, H.O. Ho, J. Control Release **89**, 57 (2003). doi:10.1016/S0168-3659(03)00091-9
21. P. Vande Witte, P.J. Dijkstra, J.W.A. Van Berg, J. Feijen, J Membr Sci **117**, 1 (1996). doi:10.1016/0376-7388(96)00088-9
22. P. Vande Witte, H. Esslbrugge, P.J. Dijkstra, J.W.A. Vanden Berg, J. Feijen, J. Membr. Sci. **113**, 223 (1996). doi:10.1016/0376-7388(95)00068-2
23. A.J. Mchugh, J. Control Release **109**, 211 (2005). doi:10.1016/j.jconrel.2005.09.038
24. S.M. Herbig, J.R. Cardinal, R.W. Korsmeyer, K.L. Smith, J. Control Release **35**, 127 (1995). doi:10.1016/0168-3659(95)00028-7

25. D. Prabakaran, P. Singh, K.S. Jaganathan, S.P. Vyas, J. Control Release **95**, 239 (2004). doi:10.1016/j.jconrel.2003.11.013
26. M.T.A. Ende, L.A. Miller, Pharm. Res. **24**, 288 (2007). doi:10.1007/s11095-006-9142-y
27. S.L. De Guevara-Fernandez, C.V. Ragel, M. Vallet-Regi, Biomaterials **24**, 4037 (2003). doi:10.1016/S0142-9612(03)00279-5
28. A. Ravaglioli, A. Krajewski, G.C. Celotti, A. Piancastelli, B. Bacchini, L. Montanari, G. Zama, L. Piombi, Biomaterials **17**, 617 (1996). doi:10.1016/0142-9612(96)88712-6
29. C. Rey, A. Hina, A. Tofighi, M.J. Glimcher, Cells Mater. **5**, 345 (1995)
30. A. Bigi, E. Boanini, S. Panzavolta, N. Roveri, Biomacromolecules **1**, 752 (2000). doi:10.1021/bm0055854
31. C.X. Wang, M. Wang, X. Zhou, Biomaterials **24**, 3069 (2003). doi:10.1016/S0142-9612(03)00154-6
32. L.L. Hench, R.J. Splinter, W.C. Allen, T.K. Greenlee, J. Biomed. Mater. Res. **2**, 117 (1971). doi:10.1002/jbm.820050611
33. L.L. Hench, J. Am. Ceram. Soc. **81**, 1705 (1998)
34. M.B. Yaylaoglu, P. Korkusuz, U. Ors, F. Korkusuz, V. Hasirci, Biomaterials **20**, 711 (1999). doi:10.1016/S0142-9612(98)00199-9
35. H.W. Kim, H.E. Kim, V. Salih, Biomaterials **26**, 5221 (2005). doi:10.1016/j.biomaterials.2005.01.047